J. Biochem. 125, 202-209 (1999)

Mutational Analysis of the Reactive Site Loop of *Streptomyces* Metalloproteinase Inhibitor, SMPI

Kazumi Hiraga,* Sailaja S. Seeram,* Shin-ichi Tate,† Naoki Tanaka,‡ Masatsune Kainosho,† and Kohei Oda*,[1]

*Department of Applied Biology, Faculty of Textile Science, Kyoto Institute of Technology, Kyoto 606-8585; †Department of Chemistry, Faculty of Science, Tokyo Metropolitan University, 1-1 Minamiohsawa, Hachioji, Tokyo 192-0364; and ‡Department of Polymer Science and Engineering, Kyoto Institute of Technology, Kyoto 606-8585

Received August 31, 1998; accepted October 12, 1998

***Streptomyces* metalloproteinase inhibitor (SMPI) is the only inhibitor to show "standard mechanism inhibition" against metalloproteinases. SMPI is a globular protein with an exposed loop containing the reactive site, C64-V65. To analyze the importance of basic residues in the reactive site loop of SMPI, mutants were constructed for R60, K61, and R66 (R60A, K61A, R66A, R60/K61A, 60/61/66A, and 60/61/66E). The mutants involving only R60, K61, and R60/K61 residues, respectively, showed strong inhibitory activity and were stable against enzyme activity. Both the triple mutants showed very weak inhibitory activity and underwent rapid degradation. The addition of basic residues to the loop (V62R and T63R) did not cause any further increase in inhibitory activity. These results suggest that basic residues in the reactive site loop play some role in maintaining a stable enzyme-inhibitor complex. The R66 mutant showed reduced activity and was rapidly degraded by enzymes. It was concluded that R66 is essential for maintaining a strong hydrophobic interaction with the S1′ hydrophobic pocket of the enzyme. To investigate the roles of the disulfide bridge and the P68 residue near the reactive site, C64/69S and P68T mutants were constructed. These mutants showed very weak inhibitory activity and were rapidly degraded by enzymes. These results suggest that the disulfide bridge and P68 residue are very essential for SMPI to function as an inhibitor.**

Key words: basic residues, disulfide bridge, metalloproteinase, reactive site loop, SMPI.

Proteinase inhibitors have been used as therapeutic agents in the treatment of diseases like AIDS and cancer. However, knowledge of these inhibitors, except for serine proteinase and HIV-proteinase inhibitors, is still inadequate. Metalloproteinases are associated with various diseases such as cancers, arthritis and hypertension. The well known metalloproteinases have been divided into two groups, the "gluzincins" and "metzincins," based on their zinc ligands (*1-5*). Gluzincins include many microbial enzymes like thermolysin and some pharmacologically important enzymes like neprilysin. Metzincins include astacins, matrix metalloproteinases, *etc.* For over twenty years drug discovery projects on metalloproteinases have relied on crystallographic data derived from thermolysin with small inhibitors, because of the paucity of the knowledge on the three-dimensional (3D) structures of metalloproteinases and their natural inhibitors. In recent years the 3D structures of many metalloproteinases and their complexes with proteinaceous inhibitors have been determined (*6-12*). Proteinaceous proteinase inhibitors are ubiquitous in nature, and play key roles in various physiological and pathological processes. For metzincin group enzymes, inhibitors have been isolated and studied for each family (*13-23*). On the other hand, for gluzincin enzyme families, only one protein inhibitor has been described, *Streptomyces* metalloproteinase inhibitor (SMPI).

SMPI, isolated from *Streptomyces nigrescens* TK-23 (*24*), is a small protein of 102 amino acid residues (*25*). It inhibits metalloproteinases like thermolysin in a 1:1 stoichiometric ratio. The SMPI gene was cloned (*26*) and the DNA sequence determined (*27*). When incubated with a catalytic amount of an enzyme, SMPI is gradually cleaved at a specific peptide bond, Cys64-Val65. This site was identified as the reactive site by mutational analysis (*28*). The reactive site of SMPI is not only hydrolyzed but also resynthesized by the target enzyme (*29*), as in the case of classical serine proteinase inhibitors, whose inhibition mechanism has been described as the standard mechanism of inhibition (*30*). SMPI is the only inhibitor exhibiting this type of inhibition mechanism against metalloproteinases. The 3D structure of SMPI has been elucidated by means of NMR techniques (*31*). SMPI is a globular protein with an exposed loop in which the reactive site is present. The

[1] To whom correspondence should be addressed: Tel: +81-75-724-7763, Fax: +81-75-724-7760, E-mail: bika@ipc.kit.ac.jp

Abbreviations: A_2pr(Dnp), N^3-(2,4-dinitrophenyl)-L-2,3-diaminopropionyl; FAGLA, 3-(2-furylacryloyl)glycyl-L-leucine amide; MOCAc, (7-methoxycoumarin-4-yl)acetyl; MMP, matrix metalloproteinase; 3D, three-dimensional; WT, wild type. Amino acid residues are represented by one-letter or three-letter abbreviations. Mutants are identified by giving the wild-type residue followed by the residue number and the substituted residue.

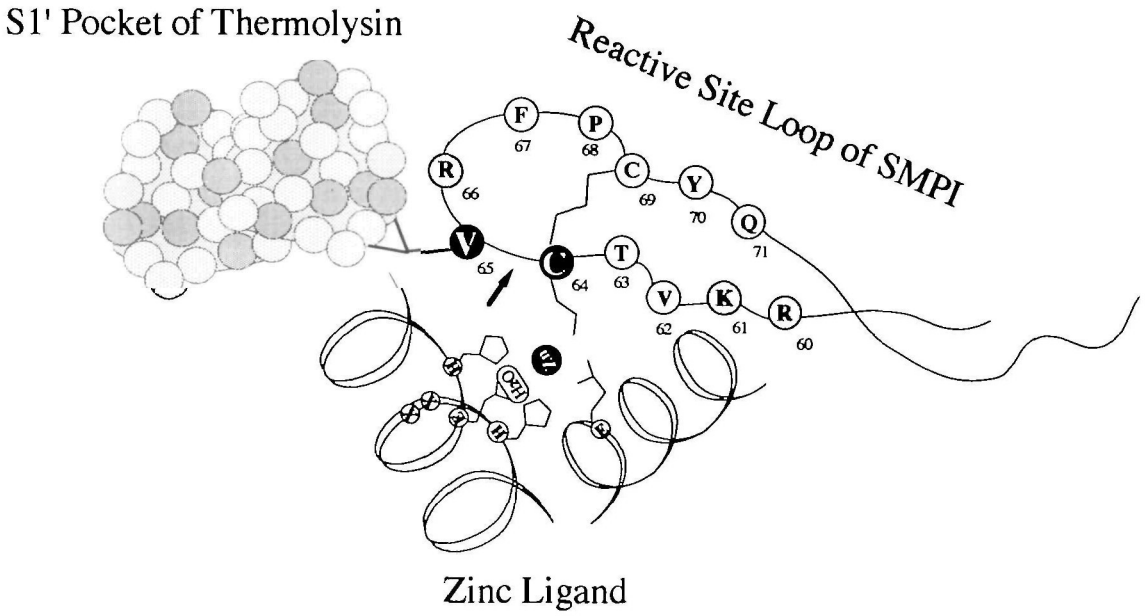

Fig. 1. **Interaction of the reactive site loop of SMPI with thermolysin.** The C64 residue interacts with the zinc ion in the active site of the enzyme. V65 interacts with the S1′ pocket of thermolysin. The arrow indicates the cleavage site.

interaction between SMPI and thermolysin was observed by producing an enzyme–inhibitor complex (*32*) by means of computer docking procedures using the crystal structure of thermolysin and the NMR-derived structure of SMPI. In the complex, as shown in Fig. 1, the carbonyl carbon of C64 (P1 residue) interacts with the catalytic zinc, and the methyl group of V65 (P1′) is in close proximity to the hydrophobic S1′ pocket of thermolysin. These results support the biochemical identification of the reactive site and the inhibition mechanism. The favorable hydrophobic interaction between the P1′ residue and the S1′ pocket of the enzyme was found to be very important for the stable complex formation on mutational analysis and also in the computer generated complex.

The basic residues, R60, K61, and R66, in the vicinity of the reactive site are thought to be essential for stable complex formation by maintaining the electrostatic interaction with the negatively charged active cleft of thermolysin. In this context, to determine the roles of these basic residues in the vicinity of the reactive site, mutational analysis was carried out.

In nature, endogenous proteinase inhibitors appear to be mostly proteins. The various requirements of a protein to act as an inhibitor are not clearly known. To some extent the rigidity and flexibility of a protein determines its ability to serve as a substrate or an inhibitor (*33*). Distinct structural elements, such as disulfide bridges, intraelectrostatic interactions, salt bridges, hydrogen bonds and buried of hydrophobic residues, are commonly seen in protein inhibitors that enhance the rigidity of their secondary and tertiary structures (*34*). SMPI has a reactive site loop and the freedom of the loop is restricted by a disulfide bridge. To understand the importance of the disulfide bridge and P68 near the reactive site, mutational analysis was also carried out.

EXPERIMENTAL PROCEDURES

Materials—A PCR kit was purchased from Perkin Elmer, Japan. All the restriction enzymes, a ligation kit, a gene-clean kit, *etc.* used were commercial products. Glutathione Sepharose 4B and CM-Sepharose CL-6B were purchased from Pharmacia Biotech AB, Uppsala, Sweden. Reduced glutathione was purchased from Wako Pure Chemical Industries, Osaka. Thermolysin was kindly donated by Daiwa Kasei, Osaka. The fluorogenic substrate, MOCAc-Pro-Leu-Gly-Leu-A_2pr(Dnp)-Ala-Arg-NH_2, was purchased from Peptide Institute, Osaka.

Construction of Mutant SMPIs—Mutants were constructed by the recombinant PCR method (*35*) as described previously (*28*), using the following mutant primers. The R60/K61/R66A mutant was constructed using the R60/K61A primer and the R66A gene as a template.

R60A(+) 5′ TACGGCCCCGCGGCGAAGGTGACC;
K61A(+) 5′ CCCGCGCGGGCGGTGACCTGCGT;
R66A(+) 5′ GTGACCTGCGTCGCCTTCCCGTGCT;
V62R(+) 5′ GCGCGGAAGCGTACCTGCGTCCGC;
T63R(+) 5′ GCGGAAGGTGAGATGCGTCCGCTTC;
60/61A(+) 5′ GGCCCCGCGGCGGCGGTGACCTG;
60/61/66E(+) 5′ GCGGAGGAGGTGACCTGCGTCGAGTTC;
C64/69S(+) 5′ TGACCAGCGTCCGCTTCCCGAGCTAC;
P68T(+) 5′ GCGTCCGCTTCACGTGCTACCAGTAC.

The mutant genes were confirmed by DNA sequencing and subcloned into the *Bam*HI and the *Sma*I sites of a pGEX expression plasmid as described previously (*28*).

Purification of Proteins—The expression and purification of the mutant proteins were carried out as described previously (*28*) or with some modification. Briefly, a bacterial sonicate was applied to a glutathione S-transferase (GST) affinity column and then the GST-SMPI

fusion protein was purified. The fusion protein was separated by thrombin digestion (25°C, 16 h). The V62R and cysteine mutant were very unstable against thrombin digestion. Hence, they were incubated with thrombin for a short time (2-4 h). The thrombin digest was subjected to CM-Sepharose column chromatography at pH 8.2 (50 mM borate buffer) and eluted with a NaCl gradient. For the basic mutants, R60A, K61A, and R66A, 50 mM phosphate buffer (pH 6.2) was used. 60/61A, 60/61/66A, and 60/61/66E did not bind to a CM-Sepharose or DEAE-Sepharose column. Hence, the thrombin digests were applied to a DEAE-Sepharose Fast Flow column in 50 mM borate buffer, pH 9.5, and the flow through (unbound fraction) solution was collected (Glutathione S-transferase and thrombin were removed *i.e.*, completely bound to the column). The samples were dialyzed and freeze-dried.

Inhibition Analysis—The inhibitory activity was analyzed using the fluorogenic substrate, MOCAc-Pro-Leu-Gly-Leu-A_2pr(DNP)-Ala-Arg-NH_2 (*36*), in 25 mM PIPES, 2 mM $CaCl_2$ buffer (pH 7.0), at 25°C. Thermolysin (1 nM) and various concentrations of an inhibitor [R60A, K61A, and T63R (0.2-3 nM); V62R (2-30 nM); R66A (4-60 nM); 60/61A (0.4-6 nM); and 60/61/66A (20-300 nM)] were incubated for 15 min, and then the residual enzyme activity was measured with a Hitachi F-2000 fluorescence spectrophotometer at λ_{ex} 323 nm and λ_{em} 398 nm. The K_i values were calculated as described previously (*28*), by nonlinear least-squares analysis (*37*).

The inhibitory activity of weak inhibitors was calculated by measuring the amount of inhibitor required to give 50% inhibition (IC_{50}) of the enzyme. The enzyme (1 nM) and various amounts of an inhibitor were mixed briefly and then the residual enzyme activity was measured. Approximate IC_{50} values were calculated.

Limited Proteolysis—The stability of the proteins against the enzyme was analyzed by Tricine-SDS-PAGE (*38*). Thermolysin (100 pmol) and inhibitors (10 nmol), E:I = 1:100 ratio, were incubated in 25 mM Tris-HCl, 2 mM $CaCl_2$ buffer (pH 7.5) at 25°C. Aliquots were withdrawn at various intervals and then subjected to Tricine-SDS-PAGE after reduction with 2-mercaptoethanol.

CD Spectra—CD spectra were taken in 50 mM Tris-HCl (pH 7.0) at 25°C using a 0.1 cm path length cell in the far UV region (190-250 nm) with a Jasco J-720 model CD spectropolarimeter as described previously (*29*). The temperature dependence of the CD intensity of C64/69S and WT was measured at 206 nm. The temperature was controlled by circulating thermostatically controlled water through the water jacket of the cell. The protein concentration was kept at about 25 μM.

NMR Experiments—Samples (100 μM) were prepared by dissolving the lyophilized proteins in 50 mM CD_3COOD, pH 5.6, buffer (Aldrich). NMR spectra were acquired with a Bruker ARX-500 spectrometer operating at 500 MHz with a custom-built high-resolution ^{1}H NMR probe.

TABLE I. **Calculated K_i values and IC_{50} values for mutants against thermolysin.** K_i values were calculated as described under "EXPERIMENTAL PROCEDURES."

Inhibitor	K_i (M)	IC_{50} values
WT	1.14×10^{-10}	0.6 nM
R60A	2.02×10^{-10}	
K61A	3.08×10^{-10}	
R60/K61A	6.11×10^{-10}	
R66A	1.19×10^{-8}	
60/61/66A	2.13×10^{-8}	
60/61/66E		5 μM
T63R	1.01×10^{-10}	
V62R	6.72×10^{-9}	
C64/69S		1.8 μM
P68T	6.17×10^{-8}	

RESULTS

To understand the importance of the basic residues and the disulfide bridge in the vicinity of the reactive site of SMPI, mutational analysis was carried out. R60, K61, and R66 were substituted with alanine (R60A, K61A, R66A, double mutant R60/K61A, and triple mutant 60/61/66A), and glutamic acid (60/61/66E, a triple mutant). V62 and T63 were changed to Arg (V62R and T63R). To understand the importance of the disulfide bridge and the Pro residue near the reactive site, C64 and C69 were substituted with Ser (C64/69S, double mutant), and Pro 68 was substituted with Thr. The mutant proteins were purified according to the nature of the mutant and approximately 5 mg protein was obtained from 2 liters of M9 medium. The P68T mutant was very poorly expressed, only 0.5 mg protein being obtained from 6 liters of culture. The mutational analysis was carried out as to two aspects, (i) inhibition and (ii) stability against enzyme.

1) Inhibition Analysis—The calculated K_i values are presented in Table I. The T63R, R60A, K61A, and R60/K61A mutants showed strong inhibitory activities. R60A, K61A, and R60/K61A showed approximately 2, 2.5, and 5 times weaker inhibitory activity, respectively, then compared with the WT inhibitor. V62R, R66A, 60/61/66A, and

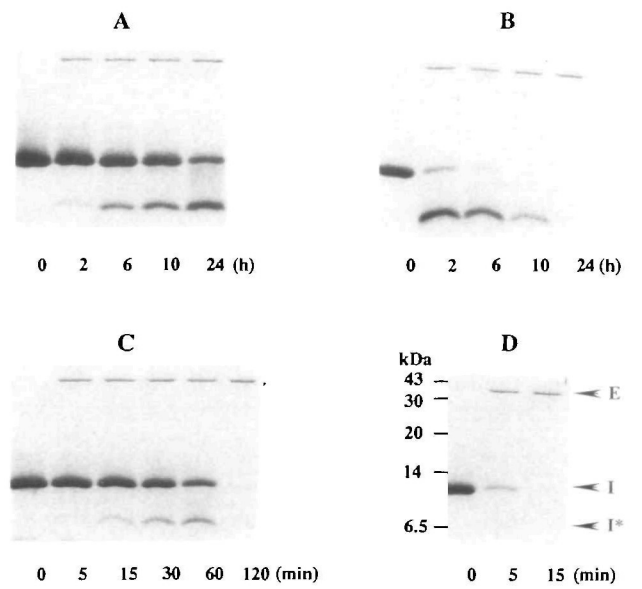

Fig. 2. **Limited proteolysis patterns of basic-residue mutants with thermolysin.** The Tricine-SDS-PAGE patterns were of 4 types. (A) WT, R60A, K61A and R60/K61A; (B) R66A; (C) 60/61/66A; and (D) 60/61/66E. The details are given under "RESULTS AND DISCUSSION." E, enzyme; I, inhibitor; I*, N-terminal fragment of the cleaved inhibitor. The C-terminal fragment disappeared during destaining of the gels.

P68T showed approximately 60, 100, 200, and 500 times weaker inhibition than the WT inhibitor, respectively. The inhibitory activity of the other mutants was analyzed by calculating IC_{50} values. The C64/69S and 60/61/66E mutants showed 4 orders of magnitude weaker inhibition compared to that of the WT inhibitor.

2) Limited Proteolysis—The stability of mutant inhibitors towards the enzyme was analyzed by limited proteolysis. The Tricine-SDS-PAGE patterns for the basic residue-mutants were of 4 types, as shown in Fig. 2. R60A, K61A and R60/K61A showed similar cleavage patterns (Fig. 2A) to that of the WT inhibitor and were stable until 24 h. Figure 2B shows the cleavage pattern of R66A, which was stable up to 10 h and then degraded by the enzyme. 60/61/66A underwent rapid degradation, no protein being seen after 1 h (Fig. 2C). 60/61/66E was the most unstable, it being degraded within 15 min incubation (Fig. 2D).

T63R was stable up to 24 h, but the cleavage was fast (Fig. 3A). V62R (Fig. 3B) was also unstable and underwent degradation before 6 h. C64/69S (Fig. 3C) underwent degradation within 5 min. The P68T mutant was degraded

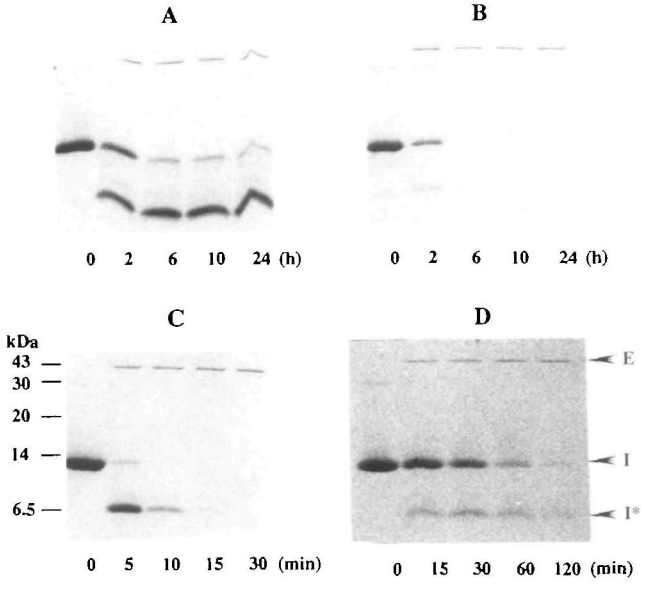

Fig. 3. **Limited proteolysis patterns of T63R, V63R, C64/69S, and P68T with thermolysin.** (A) T63R; (B) V62R; (C) C64/69S; and (D) P68T. For the details see "RESULTS AND DISCUSSION." I, inhibitor; I*, N-terminal fragment of the cleaved inhibitor. The C-terminal fragment disappeared during destaining of the gels.

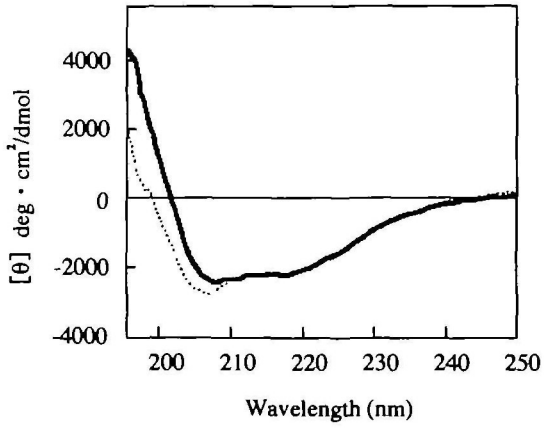

Fig. 4. **CD spectra of the WT and C64/69S inhibitors.** The spectra were taken with 25 μM inhibitors at 25°C in 50 mM Tris-HCl (pH 7.0) buffer. Data were collected in the far UV region. (·····) WT; (- - -) C64/69S.

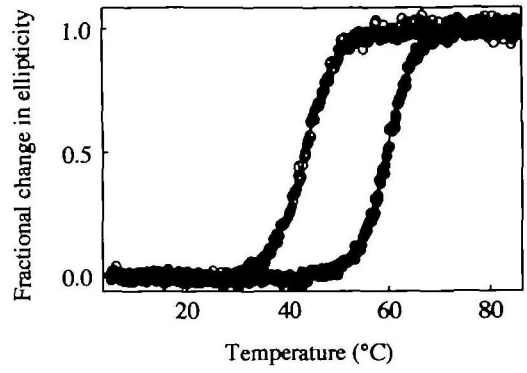

Fig. 5. **Temperature dependence of the fractional changes in ellipticity of the wild type and the C64/69S mutant.** The spectra were taken with 25 μM inhibitors at various temperatures in 50 mM Tris-HCl (pH 7.0) buffer at 202 nm. (●) WT; (○) C64/69S.

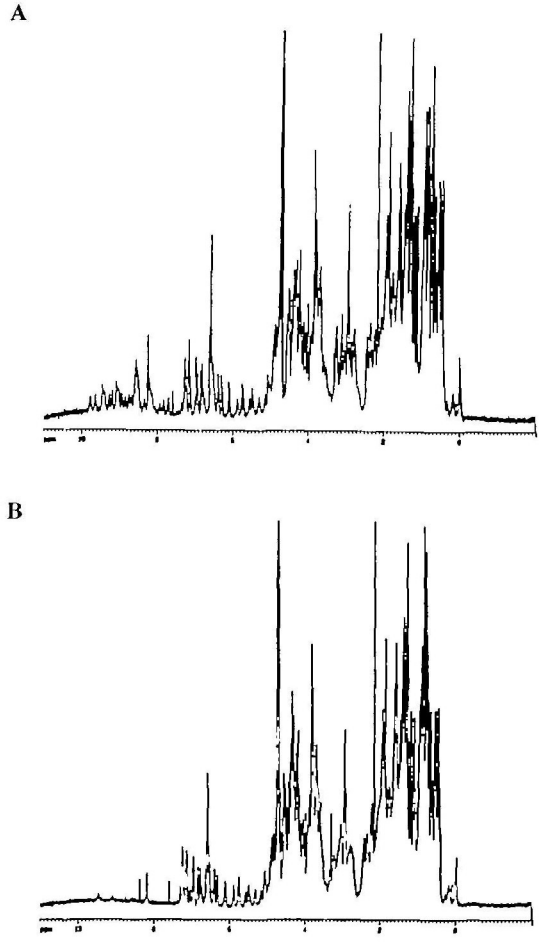

Fig. 6. **NMR spectra of the wild type and the C64/69S mutant.** Panel A, WT inhibitor, and panel B, C64/69S mutant. The chemical shifts of the two inhibitors are almost the same.

in less than 2 h (Fig. 3D).

3) CD and NMR Experiments—The CD spectrum (Fig. 4) of the C64/69S mutant was not similar to that of WT. A comparison of the fractional changes in ellipticity between WT and C64/69S mutant at various temperatures is shown in Fig. 5. The melting temperature (T_m) of WT SMPI is 59.5°C, whereas that of C64/69S is 44.0°C. In NMR experiments (Fig. 6) the chemical shifts of the ^1H proton peaks of both the proteins were nearly same.

DISCUSSION

The 3D structures of many serine proteinase inhibitors have been elucidated. In general, such inhibitors contain an exposed loop by which they interact with an enzyme. Each group of inhibitors has a different stabilization mechanism. Most serine proteinase inhibitors contain a disulfide bridge near the reactive site. Chymotrypsin inhibitor 2 and eglin c lack disulfide bonds, so the rigidity of the reactive site loop is provided by the side chains of two Arg residues (*39, 40*). These structural elements have different degrees of importance in different inhibitors. In the case of SSI (*Streptomyces* subtilisin inhibitor), disruption of the disulfide bridge near the reactive site resulted in reduced inhibitory activity and temporary inhibition (*41*). In contrast, a mutant BPTI (bovine pancreatic trypsin inhibitor) with the disulfide bond removed (Cys14-Cys38) showed as strong inhibition as the wild type inhibitor (*42*). An additional amino acid replacement in the hydrophobic core of the inhibitor was required to convert BPTI to a temporary inhibitor (*43, 44*).

SMPI exhibits many similarities to serine proteinase inhibitors including the presence of an extruded loop. Its conformation is maintained by a disulfide bridge. From the thermolysin-SMPI model-complex it is expected that the region from R60 to P68 of the reactive site loop of SMPI interacts with an enzyme (Fig. 1), and the basic residues in the reactive site loop could be responsible for maintaining a favorable electrostatic interaction. To determine various structural requirements of SMPI, mutational analysis was carried out.

Basic Residue Mutants—The R60A and K61A mutants showed strong inhibitory activity and their K_i values were comparable to that of the WT inhibitor. On limited proteolysis, as shown in Fig. 2A, R60A and K61A showed similar patterns of cleavage to that of WT and were stable up to 24 h. R66A showed 100 times reduced inhibitory activity. R66A (Fig. 2B) underwent degradation more rapidly and disappeared by 10 h. The triple mutant, 60/61/66A, showed 200 times weaker activity, which is not much different from that of the single mutant, R66A, and underwent degradation by 2 h. The limited proteolysis patterns (Fig. 2C) show that 60/61/66A is more unstable than R66A. 60/61/66E showed nearly 50,000 times weaker inhibitory activity than the WT inhibitor. 60/61/66E was degraded most rapidly, *i.e.* within 15 min (Fig. 2D).

From these results, initially it was thought that R66 is the only residue mainly required for the electrostatic interaction, and that K61 and R60 are of little importance. The electrostatic interaction between the negatively charged active cleft of an enzyme and the complementary positively charged reactive site loop of an inhibitor is essential for the stable complex formation, and negatively charged residues are not tolerated in the reactive site loop. To confirm these experimental results, the SMPI-thermolysin model-complex was observed more closely.

An extracted view of the interactions of various residues in the enzyme and the inhibitor is shown in Fig. 7 (*32*). The pink colored residues are the acidic residues, E143, D150, E166, and D226, of thermolysin. The blue colored residues are the basic residues, R60, K61, and R66, of SMPI. In this figure it can be clearly seen that three acidic residues are present in the active cleft of thermolysin, which are very close to the basic residues, R60 and K61. To our surprise, no acidic residues of thermolysin in their model interact with R66. The acidic residue, D226, of thermolysin is around R66, but it is far away and thus no interaction can be expected. Moreover, the methylene group of R66 is in close contact with the S1′ pocket of thermolysin.

This observation suggests that a basic residue is not needed at the P2′ position and thus R66 acts as a hydrophobic residue because of its large side chain. The large side chain supports the P1′ V65 residue to properly interact with the S1′ pocket of thermolysin.

Hangauer *et al.* (*45*) proposed that the hydrophobic S1′ pocket of thermolysin interacts with the P2′ residue in addition to the P1′ residue. Many researchers analyzed the substrate preference of thermolysin at individual subsites from P3-P3′, these studies also revealing the preference for a hydrophobic residue at the P2′ position (*45-47*). The natural inhibitors of thermolysin, phosphoramidon and talopeptin, also have a hydrophobic residue, Trp, at the P2′ position. According to the results of Hersh and Morihara (*47*), the Ala residue at P2′ increased the k_{cat} value 2 times and the K_m value 4 times. The increased K_m value results in weaker binding (hence, a higher K_i value in the case of the inhibitor), and the increased k_{cat} value results in faster cleavage. Indeed, the R66A mutant showed a 100 times higher K_i value, and was cleaved fast and underwent degradation by thermolysin. All of these observations strongly suggest that R66, because of its large side chain, acts only as a hydrophobic residue, but is not needed for the electrostatic interaction. R60 and K61 could be responsible for the electrostatic balance between the enzyme and the inhibitor.

To confirm this hypothesis, the R60/K61A double mutant was constructed. This double mutant retained strong inhibitory activity and showed only 5 times weaker inhibition than the WT inhibitor (Table I). On the limited proteolysis this mutant also was stable against the enzyme and was slowly cleaved, similar to as observed for R60A and K61A (Fig. 2A). These results suggest that R60 and K61, the basic residue or the electrostatic interaction has very little effect. But, based on the data for triple mutants R60/K61/R66A and R60/K61/R66E it can be said that this interaction is necessary to maintain a stable enzyme-inhibitor complex by properly positioning the reactive site loop of the inhibitor in the active cleft of the enzyme. The active cleft of thermolysin is a long canal and SMPI contains a long extruded loop which slots into the active cleft of the enzyme. Hence, even though the charge is lost in single mutants (R60A and K61A) or R60/K61A, the overall charge on the reactive site loop may be compensated for by other residues in or around the reactive site loop, such as R66 or R55. This assumption was supported by the triple

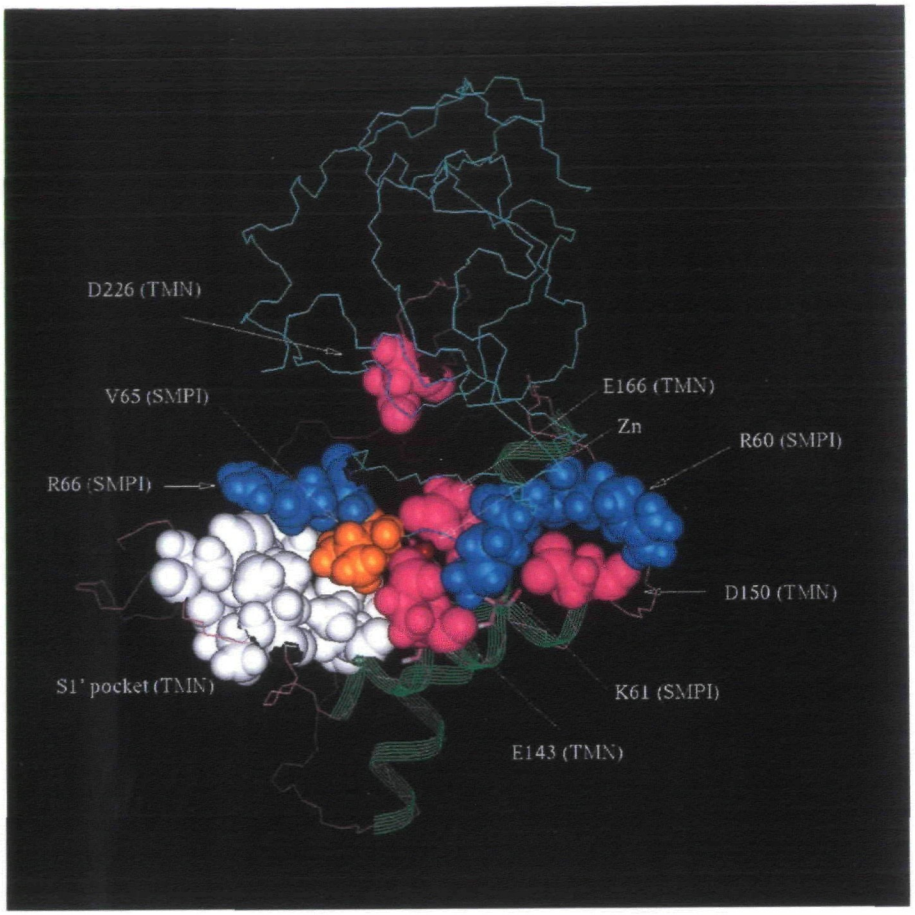

Fig. 7. **Extracted view of the interactions between basic residues in the reactive site loop of SMPI and thermolysin.** The body of thermolysin is shown as a line representation and the two α-helices are providing the Zn ligands. The acidic residues of the enzyme are presented in pink, and the S1′ site in white. The basic residues of SMPI are presented in blue, and V65 in yellow. TMN stands for thermolysin. The close contact between R66 and the S1′ site can be seen very clearly.

mutants. R60/K61/R66A was more unstable than R66A, and R60/K61/R66E was much more unstable, and it almost completely lost its inhibitory activity also.

T63R and V62R—It is expected that the inhibitory activity or strong enzyme-inhibitor complex formation could be enhanced by increasing the number of basic residues in the reactive site loop. However, stronger inhibitory activity could not be obtained by increasing the basic residues. T63R showed equal inhibitory potential to that of the WT inhibitor, but on limited proteolysis it was cleaved faster (Fig. 3A). V62R showed 60 times weaker inhibitory activity. On limited proteolysis, V62R (Fig. 3B) was degraded very rapidly by the enzyme. These results suggest that additional charged residues are not needed, or rather they may result an unfavorable interaction. In the V62R mutant, there are three consecutive basic residues (R60, K61, and R62). In the WT inhibitor, R60 and K61 are thought to be necessary for a favorable interaction and to position the reactive site loop properly in the active cleft of thermolysin. In the case of V62R, the Arg residue might misguide the reactive site loop and thus might result in a frame shift interaction of the loop with the active site of thermolysin, leading to the mismatched interactions and destabilization of the complex.

Based on these results it can be concluded that a hydrophobic residue is preferred at the P2′ position and that the side chain of R66 serves as a hydrophobic molecule. Basic residues in the reactive site loop might play some role in the complex formation by maintaining the electrostatic interaction and by guiding the reactive site loop to properly interact with the active cleft of the enzyme. Additional charged residues in the reactive site loop could lead to destabilization of the complex.

Cys Mutant—Disruption of the disulfide bridge resulted in severe loss (four orders of magnitude) of the inhibitory activity. For this mutant calculation of the K_i values was not possible, so the IC_{50} value was calculated immediately after mixing the enzyme and the inhibitor (without incubation with the enzyme). On limited proteolysis (Fig. 3C), this inhibitor underwent degradation in less than 15 min. This suggests that the Cys mutant exhibited affinity for the enzyme (even though it was very low), but mainly it lost its stability against the enzyme. The Cys mutant is easily accessible for proteolytic cleavage, and the disulfide bridge is very essential for maintaining the rigidity of the reactive site loop and the stability of SMPI against the enzyme. To check the folding and conformation of the Cys mutant, CD spectra were taken in the far UV region (Fig. 4). We also checked the thermal stability of the C64/69S mutant by means of CD spectroscopy (Fig. 5). The spectral patterns of WT and the C64/69S mutant were not similar, suggesting that there could be some disturbance in the structure of the inhibitor. The thermal stability of the C64/69S mutant was decreased by 15.5°C on removal of the disulfide bridge. However, the NMR data shows that the core structure of the mutant is not changed but almost the same to that of the wild type inhibitor (Fig. 6). Based on these results it is thought that the core body of the Cys mutant is not

influenced by disruption of the disulfide bridge, but that the reactive site loop became more flexible and lost the proper conformation. In the case of serine proteinase inhibitors, although it has been proved that the disulfide bridge or other tertiary structural features are essential for the inhibitory activity, the inhibitors are not affected drastically. However, in the case of SMPI, disruption of the disulfide bridge had drastic effect for its function and stability.

P68T—To understand the importance of P68, it was substituted with Thr. The Pro mutant showed 500 times weaker inhibitory activity and was degraded by the enzyme in less than 2 h (data not shown). Expression of the protein was also very poor. Pro68 is expected to be the essential residue for maintaining the rigidity and conformation of the reactive site loop. A proline residue is commonly observed in the vicinity of the reactive site in serine proteinase inhibitors also.

Degradation of mutant proteins by an enzyme has been observed for SMPI, some basic-residue mutants, Cys mutants, and weaker P1′ mutants. Even the native SMPI itself showed temporary inhibition. These observations suggest that SMPI has a very flexible structure, so that even a very small disturbance can also lead to instability and degradation of the inhibitor. On the other hand, this kind of flexible structure may be responsible for the wide inhibitory spectrum of SMPI. SMPI inhibited enzymes of thermolysin, mycolysin and neprilysin families of division gluzincins or clan MA. In contrast, the inhibitors of metzincin families such as TIMPs show very narrow specificity in spite of the close structural relations among those enzymes.

At present, we have little understanding of the various structural requirements of metalloproteinase inhibitors as to their inhibitory functions. In this study the importance of basic residues, a disulfide bridge and the Pro68 residue in the reactive site loop of SMPI has been revealed.

REFERENCES

1. Jiang, W. and Bond, J.S. (1992) Families of metalloendopeptidases and their relationships. *FEBS Lett.* **312**, 110-114
2. Hooper, N. (1994) Families of zinc metalloproteases. *FEBS Lett.* **354**, 1-6
3. Bode, W., Grams, F., Reinemer, P., Gomis-Ruth, F-X., Baumann, U., McKay, D.B., and Stocker, W. (1996) The metzincin-superfamily of zinc-peptidases in intracellular protein catabolism (Suzuki, K. and Bond, J., eds.) pp. 1-11, Plenum Press, New York
4. Rawlings, N.D. and Barrett, A.J. (1995) Evolutionary families of metallopeptidases in *Methods in Enzymology* (Barrett, A.J., ed.) Vol. 248, pp. 183-228, Academic Press, New York
5. Bode, W., Gomis-Ruth, F.X., and Stockler, W. (1993) Astacins, serralysins, snake venom and matrix metalloproteinases exhibit identical zinc-binding environments (HEXXHXXGXXH and Met-turn) and topologies and should be grouped into a common family, the 'metzincins.' *FEBS Lett.* **331**, 134-140
6. Gomis-Ruth, F.X., Stocker, W., Huber, R., Zwilling, R., and Bode, W. (1993) Refined 1.8 Å X-ray crystal structure of astacin, a zinc-endopeptidase from the crayfish *Astacus astacus* L. *J. Mol. Biol.* **229**, 945-968
7. Baumann, U. (1994) Crystal structure of the 50 kDa metalloprotease from *Serratia marcescens*. *J. Mol. Biol.* **242**, 244-251
8. Gomis-Ruth, F., Kress, L., and Bode, W. (1993) First structure of a snake venom metalloproteinase: a prototype for matrix metalloproteinase/collagenases. *EMBO J.* **12**, 4151-4157
9. Kumasaka, T., Yamamoto, M., Moriyama, H., Tanaka, N., Sato, M., Katsube, Y., Yamakawa, Y., Omori-Satoh, T., Iwanaga, M., and Ueki, T. (1996) Crystal structure of H_2-proteinase from the venom of *Trimeresurus flavoviridis*. *J. Biochem.* **119**, 49-57
10. Stams, T., Spurlino, J.C., Douglas, L.S., Robert, C.W., Thau, F., Ho, M., Qoronfleh, W., Tracey, M., Banks, M., and Rubin, B. (1994) Structure of human neutrophil collagenase reveals large S1′ specificity pocket. *Struct. Biol.* **1**, 119-123
11. Baumann, U., Bauer, M., Letoffe, S., Delepelaire, P., and Wandersman, C. (1995) Crystal structure of a complex between *Serratia marcescens* metallo-protease and an inhibitor from *Erwinia crysanthemi*. *J. Mol. Biol.* **248**, 653-661
12. Gomis-Ruth, F., Maskos, K., Betz, M., Bergner, A., Huber, R., Suzuki, K., Yoshida, N., Nagase, H., Brew, K., Bourenkov, G.P., Bartunik, H., and Bode, W. (1997) Mechanism of inhibition of the human matrix metalloproteinase stromelysin-1 by TIMP-1. *Nature* **389**, 77-81
13. Letoffe, S., Delepelaire, P., and Wandersman, C. (1989) Characterization of a protein inhibitor of extracellular proteases produced by *Erwinia chrysanthemi*. *Mol. Microbiol.* **3**, 79-86
14. Dugong, F., Lazdunski, A., Cami, B., and Murgier, M. (1992) Sequence of a cluster of genes controlling synthesis and secretion of alkaline protease in *Pseudomonas aeruginosa*: relationships to other secretory pathways. *Gene* **121**, 47-54
15. Suh, Y. and Benedik, M.J. (1992) Production of active *Serratia marcescens* metalloprotease from *Escherichia coli* by α-hemolysin HlyB and HlyD. *J. Bacteriol.* **174**, 2361-2366
16. Kim, K.S., Kim, T.U., Kim, I.J., Byun, S.M., and Shin, Y.C. (1995) Characterization of a metalloprotease inhibitor protein (SmaPI) of *Serratia marcescens*. *Appl. Environ. Microbiol.* **61**, 3035-3041
17. Cawston, T.E. (1986) Protein inhibitors of metalloproteinases in *Proteinase Inhibitors* (Barrett, A.J. and Salvensen, G., eds.) pp. 589-610, Elsevier, Amsterdam
18. Woessner, J.F. (1991) Matrix metalloproteinases and their inhibitors in connective tissue remodeling. *FASEB J.* **5**, 2145-2154
19. Leco, K.J., Apte, S.S., Taniguchi, G.T., Hawkes, S.P., Khokha, R., Schultz, G.A., and Edwards, D.R. (1997) Murine tissue inhibitor of metalloproteinases-4 (Timp-4): cDNA isolation and expression in adult mouse tissues. *FEBS Lett.* **401**, 213-217
20. Osthues, A., Knauper, V., Oberhoff, R., Reinke, H., and Tschesche, H. (1992) Isolation and characterization of tissue inhibitors of metalloproteinases (TIMP-1 and TIMP-2) from human rheumatoid synovial fluid. *FEBS Lett.* **296**, 16-20
21. Apte, S.S., Olsen, B.R., and Murphy, G. (1995) The gene structure of tissue inhibitor of metalloproteinases (TIMP)-3 and its inhibitory activities define the distinct TIMP gene family. *J. Biol. Chem.* **270**, 14313-14318
22. Catanese, J.J. and Kress, L.F. (1992) Isolation from opossum serum of a metalloproteinase inhibitor homologous to human α1B-glycoprotein. *Biochemistry* **31**, 410-418
23. Yamakawa, Y. and Omori-Satoh, T. (1992) Primary structure of the antihemorrhagic factor in serum of the Japanese habu: a snake venom metalloproteinase inhibitor with a double-headed cystatin domain. *J. Biochem.* **112**, 583-589
24. Oda, K., Koyama, T., and Murao, S. (1979) Purification and properties of a proteinaceous metallo-proteinase inhibitor from *Streptomyces nigrescens* TK-23. *Biochim. Biophys. Acta* **571**, 147-156
25. Murai, H., Hara, S., Ikenaka, T., Oda, K., and Murao, S. (1985) Amino acid sequence of *Streptomyces* metallo-proteinase inhibitor from *Streptomyces nigrescens* TK-23. *J. Biochem.* **97**, 173-180
26. Tanaka, K., Saito, H., Arai, M., Murao, S., and Takahashi, H. (1988) Cloning and expression of the metallo-proteinase inhibitor (S-MPI) gene from *Streptomyces nigrescens*. *Biochem. Biophys. Res. Commun.* **155**, 487-492
27. Tanaka, K., Aoki, H., Oda, K., Murao, S., Saito, H., and Takahashi, H. (1990) Nucleotide sequence of the gene for a metalloproteinase inhibitor of *Streptomyces nigrescens* (SMPI). *Nucleic Acids Res.* **18**, 6433

28. Seeram, S.S., Hiraga, K., Saji, A., Tashiro, M., and Oda, K. (1997) Identification of reactive site of a proteinaceous metalloproteinase inhibitor from *Streptomyces nigrescens* TK-23. *J. Biochem.* **121**, 1088-1095
29. Seeram, S.S., Hiraga, K., and Oda, K. (1997) Resynthesis of reactive site peptide bond and temporary inhibition of *Streptomyces* metalloproteinase inhibitor. *J. Biochem.* **122**, 788-794
30. Laskowski, M., Jr. and Kato, I. (1980) Protein inhibitors of proteinases. *Annu. Rev. Biochem.* **49**, 593-626
31. Ohno, A., Tate, S., Seeram, S.S., Hiraga, K., Swindells, M.B., Oda, K., and Kainosho, M. (1998) NMR structure of *Streptomyces* metalloproteinase inhibitor, SMPI, isolated from *Streptomyces nigrescens* TK-23-another example of ancestral $\beta\gamma$-crystallin precursor structure. *J. Mol. Biol.* **282**, 421-433
32. Tate, S., Ohno, A., Seeram, S.S., Hiraga, K., Oda, K., and Kainosho, M. (1998) Elucidation of the mode of interaction of thermolysin with a proteinaceous metalloproteinase inhibitor, SMPI, based on a model complex structure and a structural dynamics analysis. *J. Mol. Biol.* **282**, 435-446
33. Janin, J. and Chothia, C. (1990) The structure of protein-protein recognition sites. *J. Biol. Chem.* **265**, 16027-16030
34. Bode, W. and Huber, R. (1992) Natural protein proteinase inhibitors and their interaction with proteinases. *Eur. J. Biochem.* **204**, 433-451
35. Higuchi, R. (1990) Recombinant PCR in *PCR Protocols: A Guide to Methods and Applications* (Innis, M.A., Gelfand, D.H., Sninsky, J.J., and White, T.J., eds.) pp. 177-183, Academic Press, New York
36. Knight, C.G., Willenbrock, F., and Murphy, G. (1992) A novel coumarin-labelled peptide for sensitive continuous assays of the matrix metalloproteinases. *FEBS Lett.* **296**, 263-266
37. Tashiro, M., Kihira, Y., Katayama, Y., and Maki, Z. (1989) Purification and characterization of a major trypsin inhibitor, FMTI-II, from foxtail millet grain. *Agric. Biol. Chem.* **53**, 443-451
38. Ploug, M., Jensen, A.L., and Barkholt, V. (1989) Determination of amino acid compositions and NH_2-terminal sequences of peptides electroblotted onto PVDF membranes from tricine-sodium dodecyl sulfate-polyacrylamide gel electrophoresis: Application to peptide mapping of human complement component C3. *Anal. Biochem.* **181**, 33-39
39. McPhalen, C.A., Svendsen, I., Janassen, I., and James, M.N.G. (1985) Crystal and molecular structure of chymotrypsin inhibitor 2 from barley seeds in complex with subtilisin novo. *Proc. Natl. Acad. Sci. USA* **82**, 7242-7246
40. Bode, W., Papamokos, E., Musil, D., Seemuller, U., and Fritz, H. (1986) Refined 1.2 Å crystal structure of the complex formed between subtilisin Carlsberg and the inhibitor eglin c. Molecular structure of eglin c and its detailed interaction with subtilisin. *EMBO J.* **5**, 813-818
41. Kojima, S., Kumagai, I., and Miura, K. (1993) Requirement for a disulfide bridge near the reactive site of protease inhibitor SSI (*Streptomyces* subtilisin inhibitor) for its inhibitory action. *J. Mol. Biol.* **230**, 395-399
42. Marks, C.B., Naderi, H., Kosen, P.A., Kuntz, I.D., and Anderson, S. (1987) Mutants of bovine pancreatic trypsin inhibitor lacking cysteine 14 and 38 can fold properly. *Science* **235**, 1370-1373
43. Coplen, L.J., Frieden, R.W., and Goldenberg, D.P. (1990) A genetic screen to identify variants of bovine pancreatic trypsin inhibitor with altered folding energetics. *Proteins* **7**, 16-31
44. Goldenberg, D.P., Berger, J.M., Laheru, D.A., Wooden, S., and Zhang, J.X. (1992) Genetic dissection of pancreatic trypsin inhibitor. *Proc. Natl. Acad. Sci. USA* **89**, 5083-5087
45. Hangauer, D.G., Monzingo, A.F., and Matthews, B.W. (1984) An interactive computer graphics study of thermolysin-catalyzed peptide cleavage and inhibition by *N*-carboxymethyl dipeptides. *Biochemistry* **23**, 5730-5741
46. Pozsgay, M., Michaud, C., and Orlowski, M. (1985) The active site of endopeptidase-24.11: substrate and inhibitor studies. *Biochem. Soc. Trans.* **13**, 44-47
47. Hersh, L.B. and Morihara, K. (1986) Comparison of the subsite specificity of the mammalian neutral endopeptidase 24.11 (enkephalinase) to the bacterial neutral endopeptidase thermolysin. *J. Biol. Chem.* **261**, 6433-6437